ISSN 1021-4437, Russian Journal of Plant Physiology, 2018, Vol. 65, No. 5, pp. 658–666. © Pleiades Publishing, Ltd., 2018.
Original Russian Text © V.E. Sofronova, T.K. Antal, O.V. Dymova, T.K. Golovko, 2018, published in Fiziologiya Rastenii, 2018, Vol. 65, No. 5, pp. 331–339.

RESEARCH PAPERS

Seasonal Changes in Primary Photosynthetic Events during Low Temperature Adaptation of *Pinus sylvestris* in Central Yakutia

V. E. Sofronova[a], *, T. K. Antal[b], O. V. Dymova[c], and T. K. Golovko[c]

[a] *Institute for Biological Problems of the Cryolithozone, Siberian Branch, Russian Academy of Sciences, Yakutsk, 677000 Russia*
[b] *Moscow State University, Moscow, 119991 Russia*
[c] *Institute of Biology, Komi Research Center, Ural Branch, Russian Academy of Sciences, Syktyvkar, 167000 Russia*
**e-mail: vse07_53@mail.ru*

Received June 6, 2017

Abstract—The methods of chlorophyll fluorescence induction and HPLC were used to study the influence of autumnal temperature decrease on photochemical electron-transport activity of photosystem II (PSII), nonphotochemical quenching of excessive excitation energy, and the composition of pigments in the first-year needles of *Pinus sylvestris* L. trees grown naturally in Central Yakutia. In the period from the beginning of September to October 10, the chlorophyll content was reduced by half, while the Chl *a*/*b* ratio increased from 2.9 to 4.3–4.5, indicating the degradation of peripheral antenna complexes. The decrease in average daily temperature to 4.9–6.4°C led to a transient increase in the quantum yield of nonphotochemical quenching (ΔpH-dependent parameter ϕ_{NPQ}). These changes were accompanied by a slow accumulation of unregulated zeaxanthin fraction insensitive to illumination conditions. The further decrease in average daily temperature to near-zero levels was paralleled by a sharp increase in zeaxanthin content, while the pH-dependent quenching was replaced with the constitutive quenching (parameter $\phi_{f,D}$) because of the supposed structural reorganization of PSII. These processes were accompanied by a fast decrease in PSII functional activity, which was mostly due to the impairment of plastoquinone photochemical reduction. Freezing temperatures (from −3.6 to −12.1) destructed the oxygen-evolving complex in PSII and completely inactivated the PSII reaction centers. It is concluded that the largest changes in the condition of photosynthetic apparatus occur at a near-zero temperature range and proceed until complete inactivation of PSII under the action of freezing temperatures.

Keywords: Pinus sylvestris, needles, chlorophyll fluorescence, photosynthetic pigments, seasonal dynamics, low-temperature adaptation

DOI: 10.1134/S1021443718050163

INTRODUCTION

In the northerly latitudes of the temperate zone, the autumnal shortening of the daylight period and decreasing temperatures are perceived by trees as a signal for the cessation of growth and the onset of cold hardening [1]. During suppression of photosynthesis in evergreen conifers in the autumn period, the primary photosynthetic processes undergo adaptive changes that prevent the accumulation of excess light energy and generation of reactive oxygen species (ROS) in chloroplasts. The fast-operating nonphotochemical quenching (*qE*) becomes less effective during the cold season because of the retarded electron transport and low energization of the thylakoid membranes. Therefore, light-independent constitutive quenching of excitation energy in the antenna [2, 3] and the reaction centers (RC) [4] becomes particularly important. The adaptation mechanisms may include the inactivation of RC in photosystem II (PSII) as well as the structural and functional rearrangement of light-harvesting complexes (LHC). These changes facilitate strong nonphotochemical quenching (NPQ) by promoting the aggregation of LHCII proteins, the accumulation of zeaxanthin (Zea) and lutein (Lut) carotenoids featuring photoprotective and antioxidant properties, and the increased expression of PsbS and ELIP proteins [5–11]. The energy balance between PSII and PSI under natural cold adaptation in conifers is controlled through the plastoquinone (PQ) redox state, which is

Abbreviations: Car—carotenoids; β-Car—β-carotene; Chl—chlorophyll; ETC—electron-transport chain; LHC—light-harvesting complex; Lut—lutein; NPQ—nonphotochemical quenching of Chl fluorescence; OEC—oxygen-evolving complex; PAR—photosynthetically active radiation; PFD—photon flux density; PQ—plastoquinone; PSI—photosystem I; PSII—photosystem II; PSA—photosynthetic apparatus; Q_A—primary quinone acceptor of electrons in PSII; Q_B—secondary quinone acceptor of electrons; *qE*— energy dependent component of nonphotochemical quenching of Chl fluorescence; RC—reaction centers; ROS—reactive oxygen species; Vio—violaxanthin; VXC—violaxanthin cycle; Zea—zeaxanthin.

in turn significantly affected by the enhanced cyclic electron transport around photosystem I (PSI) and chlororespiration [2, 12].

Central Yakutia is characterized by a rapid autumnal decrease in temperature. Therefore, the temperature reduction proceeds steeper than the shortening of photoperiod as compared to the gradients of above parameters in geographical regions with a milder climate at the same latitude. Furthermore, Yakutia region is distinguished by extremely low winter temperatures, unrecorded anywhere else in the Northern Hemisphere (the average winter temperatures range from −32.5 to −42.5°C). These environmental conditions underlie the specificity of cold adaptation of the photosynthetic primary processes in evergreen woody plants.

Pinus sylvestris (Scots pine) is an extremely cold-resistant species [13]. Pine forests occupy 8–9% of the boreal forest area in Yakutia. Cold adaptation lasts in Central Yakutia for approximately 6–7 weeks, from the beginning of September to mid-October. The seasonal decrease of average daily temperature from 10–12°C to the freezing levels of −3 to −8°C at this timeframe and the reduction of photoperiod from 14.2 to 10 h convert the photosynthetic apparatus (PSA) to its winter condition that tolerates extremely low winter temperatures and enables the resumption of photosynthesis in early summer.

In this work, complex studies were carried out for the first time to analyze the functional inactivation of PSII, nonphotochemical quenching, and pigment composition in *P. sylvestris* needles during the formation of frost-resistant PSA in the natural conditions of Central Yakutia.

MATERIALS AND METHODS

Plant material and conditions of plant growing. *Pinus sylvestris* L. is a widespread evergreen woody species in the boreal forests of Yakutia. The present study was performed in 2014 in a forest park area at the Botanical Garden of the Institute for Biological Problems of the Cryolithozone (Siberian Branch, Russian Academy of Sciences) located on the second terrace above the flood plain of the river Lena (62°15′ N, 129°37′ E). Field samples were collected on a permanent experimental plot. The age of pine trees was 15–18 years; their heights were 3–5 m.

Air temperature at the experimental plot was recorded with a DS 1922L iBitton thermograph (Dasllas Semiconductor, United States) at 1-h intervals. The irradiance was recorded every 30 min with a LI-190 quantum sensor (LI-COR, United States). The daily incident solar radiation was determined by averaging data recorded at half-hour intervals from sunrise to sunset; the calculated photon flux density (PFD) was expressed in μmol photons per square meter per second. The average air temperature during the growth period (May–September) was 13.6°C in 2014, and the total precipitation was 145 mm. The weather conditions throughout the experiment were typical of Central Yakutia.

Measurements of chlorophyll *a* fluorescence. The seasonal dynamics of chlorophyll (Chl) fluorescence induction curves (OJIP curves) was monitored from August 23 to November 25 using a FluorPen FP 100-MAX-LM fluorometer (Photon Systems Instruments, Czech Republic). Fluorescence was assessed after 30-min dark adaptation of needles in field conditions during August–September and under laboratory conditions in October–November. The OJIP fluorescence transients were induced by a 3-s pulse of blue light (λ = 455 nm) at a PFD of 3000 μmol photon/(m^2 s). When the measurements were conducted in the laboratory, the shoots were excised 1 h prior to sunrise and transported within 30 min to the laboratory in a light-proof thermostatic container at natural air temperature. Next, fluorescence measurements were performed immediately, without adaptation of plant material to room temperature. The obtained induction curves were analyzed using parameters of the JIP test [14].

The quantum yields of PSII photochemical reaction $\phi_{PSII} = (F'_m - F_s)/F'_m$, the pH-dependent nonphotochemical quenching $\phi_{NPQ} = F_s/F'_m - F_s/F_m$, and of nonregulated losses (constitutive quenching) $\phi_{f,D} = F_s/F_m$ in the current year needles were determined with a PAM-2500 fluorometer (Walz, Germany) [15]. The minimal fluorescence (F_0) was excited in samples adapted to darkness for 30 min using the probe light pulses (PFD = 0.1 μmol photon/(m^2 s), λ = 630 nm, pulse duration 1 μs, modulation frequency 200 Hz). The maximum fluorescence yield (F_m) in dark-adapted samples was assessed by applying the probe light pulses (100 kHz modulation frequency) superimposed with the saturating light pulse. The saturating light pulse was characterized by PFD of 8000 μmol photon/(m^2 s), the maximum emission at 630 nm, and the duration of 400 ms. By measuring Chl fluorescence on light-adapted samples, the values of steady-state fluorescence F_s and maximum fluorescence F_m' were determined (measurements of F_s and F'_m are technically similar to determination of F_0 and F_m, respectively). Based on these basic parameters, the photochemical and nonphotochemical events in PSII were characterized.

In the period from July to the end of September, the above fluorescence parameters were measured in situ in the first half of a sunny day (from 11:00 to 13:00 solar time). To accomplish this, the undetached needles of the current year were adapted to darkness for 30 min, and F_m and F_0 were first determined. Then, the samples were successively illuminated for 10 min with actinic light at PFD of 5, 28, 65, 112, 190, 250, 305, 460, and 637 μmol photon/(m^2 s). At the end of

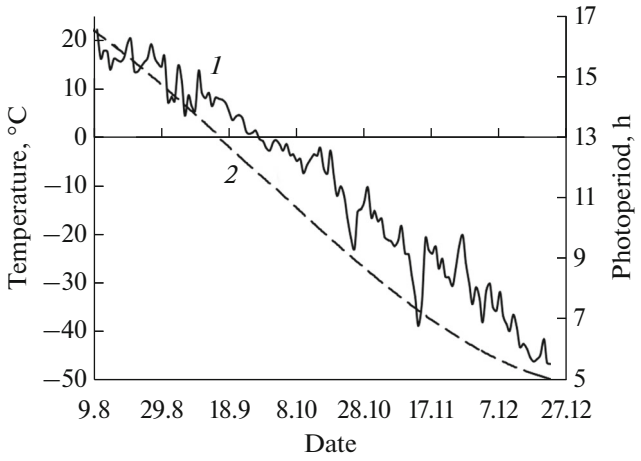

Fig. 1. Seasonal decrease in (*1*) mean daily temperature and (*2*) daylight length throughout the investigation period. Yakutsk (62°15′ N, 129°37′ E), 2014. Averaged data for day–night cycles and for the daylight period are presented. Temperature at the experimental plot was measured at a height of 2 m above the ground at 1-h intervals.

each 10-min cycle, sufficient for attaining the steady-state photosynthesis, parameters F_s and F_m' were determined. Based on these data, we calculated ϕ_{PSII}, $\phi_{f,D}$, and ϕ_{NPQ}.

Analysis of pigments. Current year needles were sampled from the middle well-lit part of the crown before the sunrise. The samples were immediately fixed in liquid nitrogen and transported in Dewar vessels to the laboratory. Photosynthetic pigments were extracted from the plant material with 100% acetone at 8–10°C under low light. The homogenate was centrifuged for 20 min at 8000 *g* at 4°C. The content of Chl and carotenoids (Car) in the supernatant was determined spectrophotometrically with an Agilent 8453E spectrophotometer (Agilent Technologies Deutschland GmbH, Germany) by recording absorbance at wavelengths of 662, 644, and 470 nm [16]. The dry weight of plant material was determined by drying parallel samples (50 mg, 3–4 replicates) to a constant weight in a drying cabinet at 100 ± 2°C.

The composition of carotenoids in the needles prefixed with liquid nitrogen was analyzed after liophylization of samples with a VirTis freeze dryer (United States). The lyophilizates were stored at –80°C and used for the analysis of pigments by HPLC. Individual carotenoids were separated by the reverse phase HPLC (Knauer, Germany) with a modified method [17] after extracting the lyophilizates with 100% acetone. The calibration curves were plotted using pure standard substances (pigments) obtained from Sigma and Fluka (United States).

The data were processed by the analysis of variances (ANOVA) of the descriptive statistics at a significance level of 0.05. Statistically significant differences between independent samples were revealed using Fisher's and Duncan's tests. The table and figures show mean values and their standard deviations. Biochemical indices were determined in 3–5 replicates with two assays per replicate.

RESULTS

Experiments were carried out from the beginning of August to the end of December 2014. The average daily air temperature decreased throughout this period from 21–22°C to the range between –30 and –46°C, and the lengths of light day shortened from 17.4 to 5.1 h (Fig. 1). The average night temperatures were 3–5°C lower than the daily average values. The beginning of weak frosts was noted on the fourth week of September; persistent lowering of night temperature below 0°C level occurred after September 27. The amount of precipitation in August was 43 mm and it was 25 and 11 mm, respectively, in September and October. The snow cover was established on October 19. The thickness of snow layer was 16 cm by the middle of November and 24–26 cm in December.

The content of Chl *a* and *b* in fully developed first-year needles was found to decrease in the autumn period (Table 1). The main drop in Chl content was noted within the first three weeks of September. During this period, the daylight duration shortened from 16 to 12.7 h, while the average daily air temperature decreased from 18.5 ± 6.0 to 6.2 ± 2.3°C (Fig. 1). The average daily photosynthetically active radiation (PAR) dropped from 540 ± 120 to 380 ± 160 μmol photon/(m^2 s). In the period from September 19 to 26, the night and day temperatures were 1.6 ± 2.4 and 4.0 ± 2.3°C, respectively; the average daily PAR was 305 ± 85 μmol photon/(m^2 s). In the subsequent two weeks, the night and day temperatures decreased gradually to the freezing range, from –3.6 to –5.6°C and from –2.3 to –4.1°C, respectively (Fig. 1), while the PAR level reduced to 280 ± 85 μmol photon/(m^2 s). Under these climatic conditions corresponding to stage 2 of cold acclimation, the Chl content declined at a noticeably slower rate. The content of Chl (*a* + *b*) remained almost constant in the period after a sustained snow cover was formed (on October 19) at freezing temperatures from –18 to –46°C. The Chl *a*/*b* ratio was 2.9 in August and increased to 3.9–4.5 in September and the first half of October; this increase pointed out that Chl *b* degraded faster than Chl *a* (Table 1).

The most pronounced changes in the composition of carotenoids were observed in September (Fig. 2). The fraction of β-carotene (β-Car) in August accounted for 36% of total carotenoid content, while this fraction reduced to approximately 23% of the total Car pool in October. The main decrease in β-Car content (to 26.3%) was observed around September 25, when the average daily temperature decreased gradually from 16.3 to nearly 0°C. In the subsequent

Table 1. Content and proportions of photosynthetic pigments in the current year needles of *Pinus sylvestris*

Date	Stages of development and hardening	Chl ($a + b$), mg/g dry wt	Chl a/b	Car, mg/g dry wt	Chl/Car
16.08	Accumulation of bud weight; transition of buds to organic dormancy	2.31 ± 0.05^{a}	2.92 ± 0.03^{ab}	0.44 ± 0.01^{a}	5.16 ± 0.24^{b}
05.09	Onset of stage 1 hardening	1.72 ± 0.02^{ab}	3.23 ± 0.07^{c}	0.40 ± 0.02^{a}	4.33 ± 0.25^{a}
18.09	Stage 1 hardening	1.25 ± 0.06^{b}	3.42 ± 0.04^{bc}	0.42 ± 0.01^{a}	3.42 ± 0.04^{a}
26.09	Onset of stage 2 hardening	1.13 ± 0.05^{b}	3.94 ± 0.13^{a}	0.44 ± 0.02^{a}	2.56 ± 0.09^{a}
16.10–22.12	Completion of stage 2 hardening, enforced dormancy	0.99 ± 0.08^{b}	4.33 ± 0.20^{abc}	0.45 ± 0.03^{a}	2.23 ± 0.18^{a}

Different superscript symbols designate significant differences (Dunkan's test, $P < 0.05$).

10-day period, when air temperatures dropped to −3.5 or −4.0°C, the relative content of β-Car in the total Car pool decreased by only 2.5%. As can be seen in Fig. 2, the early autumn changes similar to those of β-Car were also typical of Lut. By the end of the third week of September, the relative content of Lut increased transiently from 44 to 54% but dropped to 48% at the end of September and to nearly 45% in the beginning of October. Nevertheless, the relative content of Lut normalized to Chl content in the antenna pigment–protein complexes was 2.3–2.5 times higher in the winter season than in summer (Table 1, Fig. 2).

The sum of xanthophylls (zeaxanthin, violaxanthin, and antheraxanthin) of the violaxanthin cycle (VXC) constituted 8–10% of the total carotenoid pool in summer and increased to 23–24% in winter. The relative content of VXC pigments remained almost constant upon the decrease in average daily temperature to 5–6°C. At the same time, the amount of Zea fraction remaining undecomposed at night increased from 1.7 to 4.2% compared to the background decrease in relative content of Vio from 6.1 to 1.9%. A sharp increase in Zea content up to 15.9%, which was ninefold larger than its relative content in August, was noted at the end of September when the average daily air temperature dropped to 2.2 ± 1.9°C and the average night temperature was 1.4 ± 0.4°C (Fig. 2). During the next ten days, the relative amount of Zea increased by another 6.8%. In total, the relative content of Zea became more than 12.9 times higher by the middle of October than in summer months.

Measurements of OJIP curves provided information on primary photosynthetic reactions in *P. sylvestris* needles (Fig. 3). The fluorescence induction curves measured at the end of August and in the beginning of September (curves *1* and *2*) comprised three clearly visible kinetic stages representing the sequential light-induced reduction of the following pools: the PSII acceptor side (OJ phase), the plastoquinone pool (JI), and the entire photosynthetic electron-transport chain (ETC), including PSI (IP) [18]. It can be seen in Fig. 3a that the initial Chl fluorescence F_0 decreased with the decrease in temperature. This is consistent with the observed reduction of total Chl content in needles (Table 1). These changes were accompanied by the decrease in the amplitude of OP rise (Fig. 3a) that quantifies the F_v/F_m parameter, the maximum photochemical efficiency of PSII.

The relative amplitude of the JP transition is a measure of the ability of PSII to reduce the plastoquinone pool (PQ) [14]. Its decrease points to the disturbance of electron transport on the acceptor or donor

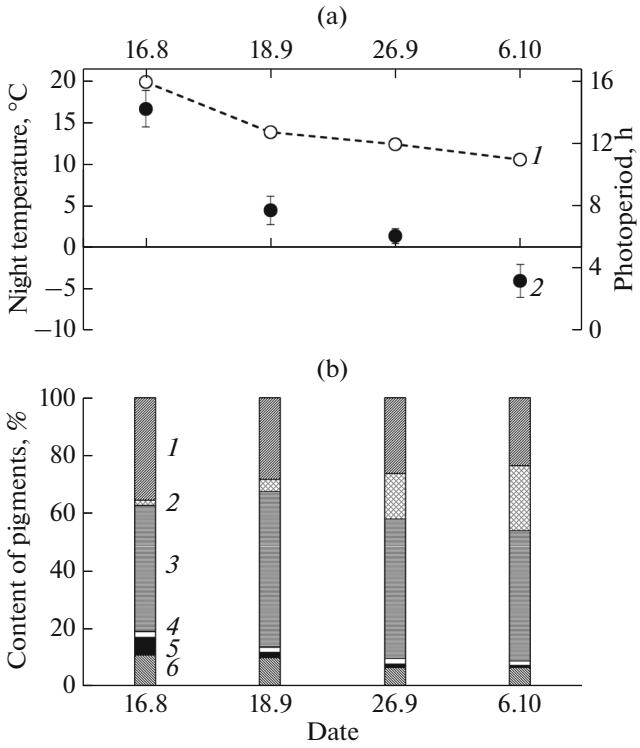

Fig. 2. (a) Seasonal decrease in photoperiod and (*1*) night temperatures (*2*) and (b) their influence on the proportions of individual carotenoids (% of total carotenoids) in the current year needles of *Pinus sylvestris*; *1*—β-carotene, *2*—zeaxanthin, *3*—lutein, *4*—antheraxanthin, *5*—violaxanthin, *6*—neoxanthin. Measurements were carried out in 2014.

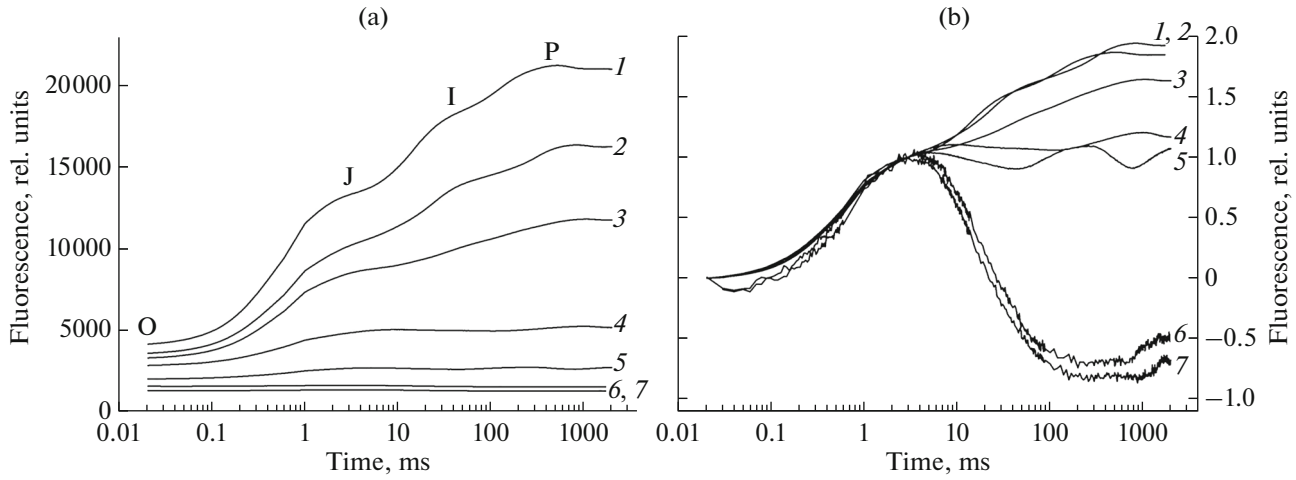

Fig. 3. Induction curves of chlorophyll fluorescence (OJIP) measured with the current year needles of *Pinus sylvestris* by means of a Fluorpen FP 100-MAX-LM, Czech Republic. (a) Original curves, (b) the induction curves normalized to the amplitude of the OJ phase (at 3 ms). Curves *1, 2, 3, 4, 5, 6, 7* represent the measurements carried out on August 23; September 9, 19, and 24; October 6 and 24; and November 25 (2014), respectively. PFD was 3000 μmol photon/(m^2 s). Measurements were carried out at ambient temperature after 30-min dark adaptation. Each curve was obtained by averaging at least five replicate measurements.

sides of PSII and indicates the accumulation of so-called Q_B-nonreducing centers of PSII. The relative extent of JP transition was estimated by normalizing the OJIP curves to the amplitude of OJ step (Fig. 3b).

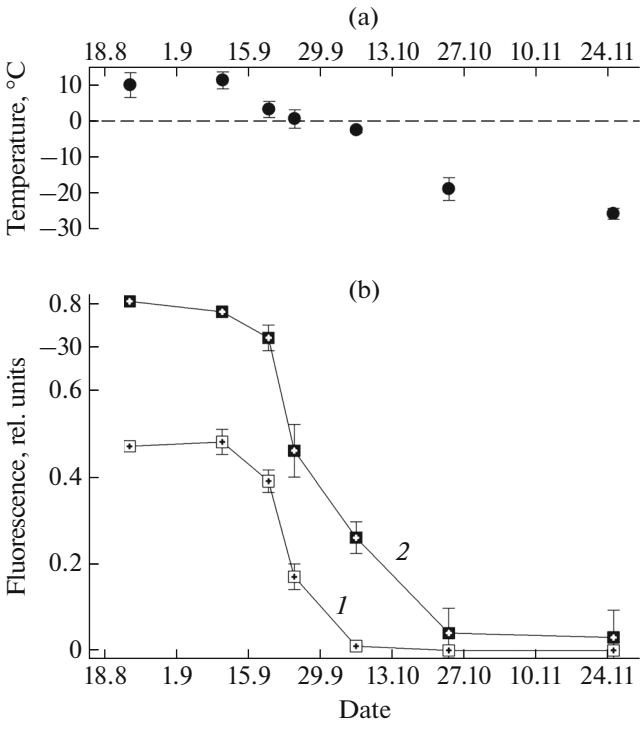

Fig. 4. Changes in (a) mean daily temperature and (b) chlorophyll fluorescence parameters during seasonal adaptation of *Pinus sylvestris*. The parameters F_v/F_m and (1 – Vj) were calculated from the curves presented in Fig. 3. *1*—(1 – Vj), *2*—F_v/F_m.

As can be seen in Fig. 3b, the highest amplitude of the JP step was observed from the end of August to the beginning of September, and then this step decreased quickly to an almost zero level by the end of September. The induction curves measured at the end of October and in November were composed of the initial rise of Chl fluorescence to the J level and the subsequent decrease of emission below the initial O level (Fig. 3b).

Figure 4 characterizes the photochemical activity of PSII (F_v/F_m) and the ability of PSII to reduce the PQ pool (the parameter (1 – Vj) quantifies the relative amplitude of the JP phase) as a function of seasonal changes in air temperature. The parameters of Chl fluorescence were automatically calculated from the curves in Fig. 3. The maximum decrease in F_v/F_m and (1 – Vj) was observed in the period from September 19 to October 6, when the temperature changed insignificantly but intersected the 0°C level (Fig. 4a). It is noteworthy that the parameter (1 – Vj) approached zero at the beginning of October, while the parameter F_v/F_m became zero at the end of October. This finding indicates that PSII first completely lost its ability to reduce the PQ pool and then lost its capacity of photochemical energy conversion; i.e., it became unable to perform the primary charge separation and reduce Q_A.

Photoprotective processes were studied by analyzing the seasonal dynamics of PSII photochemical efficiency (ϕ_{PSII}), the quantum yield of constitutive energy losses ($\phi_{f,D}$), and the quantum yield of non-photochemical quenching (ϕ_{NPQ}) during the growth of needles in summer and their hardening in autumn (Fig. 5). The figure shows Chl fluorescence upon steady-state photosynthesis under actinic light intensity of 250 μmol/(m^2 s). This level approximates the average

daylight irradiance in the second half of September, which varied from 150 to 460 μmol photon/(m^2 s) depending on the density of clouds. Similar seasonal changes of Chl fluorescence parameters were also observed at other actinic light intensities within the aforementioned range.

Shortening of the photoperiod and the autumnal cooling induced a gradual decrease in the parameter ϕ_{PSII} from 0.7 in summer to 0.4 in September and a subsequent faster decrease to 0.2 when the temperature approached the zero level. The parameter ϕ_{NPQ} was 0.09 in early August but it increased to 0.18–0.20 in the fourth week of August. The maximum ϕ_{NPQ} values (0.32–0.34) were observed in the second half of September when the average daily temperature was 1–6°C. The subsequent lowering of average daily temperature to 1 or −3°C was accompanied by a sharp decrease in ϕ_{NPQ} (Fig. 5). The parameter $\phi_{f,D}$ designating constitutive nonphotochemical energy losses increased from 0.23–0.25 in mid-September to 0.68 at the end of September, when the average daily temperature dropped from 4–6°C to the range from 0 to −3°C (Fig. 5). The increase in constitutive nonphotochemical energy losses was accompanied by the accumulation of unregulated Zea fraction that remained stable at night (Fig. 2).

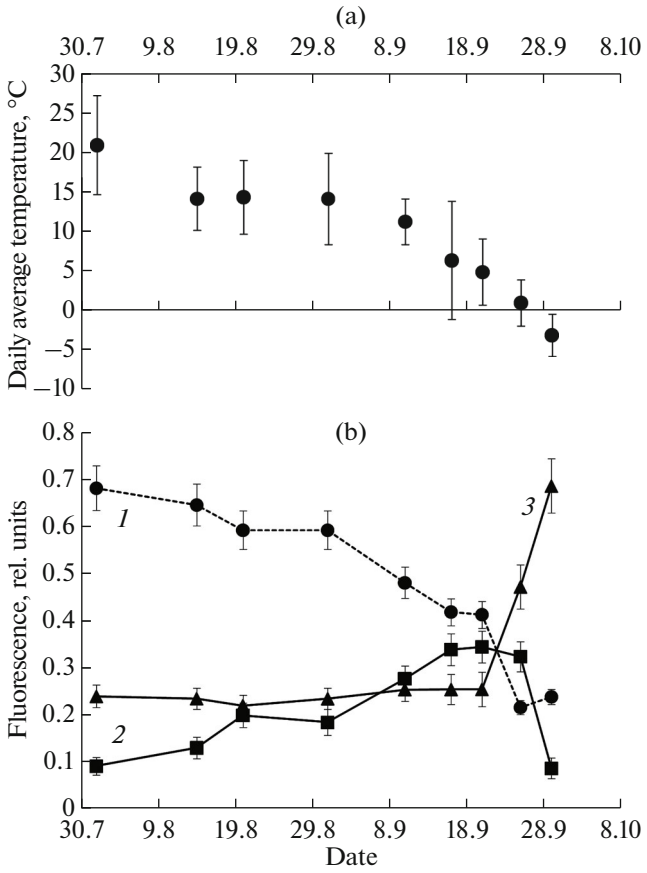

Fig. 5. Seasonal changes in (a) average daily temperature and (b) photochemical and nonphotochemical quenching in the first-year needles of *Pinus sylvestris*. The induction kinetics for ϕ_{PSII} (*1*), ϕ_{NPQ} (*2*), and $\phi_{f,D}$ (*3*) were measured under steady state condition during illumination with actinic light of 250 μmol photon/(m^2 s). Fluorescence measurements were conducted in the field on undetached needles. Data are mean values ± standard deviation (n = 3–5).

DISCUSSION

Low temperatures are known to inhibit photosynthesis, primarily Calvin cycle reactions, by promoting the accumulation of excessive reductants in the chloroplast stroma and by reducing the photosynthetic ETC carriers, including the PQ pool [2, 19]. The decomposition of starch in the chloroplasts of needle mesophyll may occur during the autumn period and contribute to the accumulation of NAD(P)H and the reduced PQ form [13]. The resulting imbalance between light reactions and photosynthetic carbon metabolism enhances the generation of ROS, namely, singlet oxygen in PSII and superoxide anion radical in PSI. Oxidative stress causes the destruction of PSA, thylakoid membranes, and other cellular components [2, 19]. These changes necessitate the structural–functional rearrangements of photosynthetic light reactions, primarily in the PSII complex, and the activation of photoprotective and regulatory mechanisms aimed at maintaining redox homeostasis and photostasis in chloroplasts by suppressing the oxidative damage. The principal photoprotective mechanisms include the decrease in activity and the absorption cross section of PSII, as well as facilitation of dissipative processes in LHC and PSII centers [2, 4–9, 11].

In the present work, we examined the development of photoprotective processes in *P. sylvestris* needles in relation to seasonal changes in temperature and photoperiod. To accomplish this, we measured the pigment composition and Chl fluorescence parameters during autumnal cold acclimation. In accordance with the theory of woody plant hardening [20], our experiments extended through all principal stages of frost hardening: the transition to dormancy that progressed first to "stage 1" hardening (at day/night temperatures of 5–12/2–6°C) and then to "stage 2" hardening (at temperatures from 0 to −10°C) as well as the winter dormancy.

The content of Chl (a + b) decreased in needles during cold adaptation by a factor of 1.8 (Table 1). The pine needles in Yakutia, unlike geographical regions with a milder climate [5–9], showed the rapid decline in Chl content in the first half of September, when the average daily temperature dropped to 5–6°C and the daylight duration shortened to 12.7–14.2 h. The lowered Chl content in needles may reflect the decay of antennal Chl-binding proteins Lhcb (PSII) and Lhca (PSI) in response to the decreasing temperature [5, 8, 9].

According to Ottander et al. [5], the content of Lhcb proteins in the peripheral antenna of *P. sylvestris* needles dropped by 40–45% in the period from September to December in pine trees grown in northern Scandinavia (63°50′ N, 20°20′ E), and this drop was accompanied by a 1.7-fold decrease in Chl content. This phenomenon resulted from downregulation of transcription and translation of the nuclear genes encoding the proteins of the Lhcb family. These regulatory changes were due to the reduction of PQ pool caused by the inhibition of Calvin cycle reactions [2, 21].

Apart from the decrease in total Chl pool, we found a predominant decrease in Chl *b* content relative to Chl *a* (Table 1). The Chl *a*/*b* ratio was 2.9 in August, and it increased by more than 1.5 times by the beginning of October. For comparison, the Chl *a*/*b* ratio for *P. sylvestris* needles in northern Scandinavia increased gradually in the period from September to December [5]. Chl *b* is an obligatory and indispensable component of the peripheral antenna in LHCII [22]. The reduced content of Chl *b* reflects the decreased size of the peripheral antenna in PSII and, consequently, the restricted flow of excitation energy to the reaction center. These constraints mitigate the imbalance between energy absorption and utilization in photosynthesis.

Our analysis revealed that the fastest drop of PSII activity occurred in the period from September 19 to October 6, when the average daily temperature decreased gradually from 3 to −3°C (Fig. 4). This period corresponds to the completion of stage 1 and the beginning of stage 2 of frost hardening, during which unbound water is released from the cells to intercellular spaces [13]. Indeed, the needles of *P. sylvestris* trees grown in Central Yakutia rapidly accumulated a 15-kD protein, dehydrin, by the end of September, and this accumulation was associated with a substantial decrease in water content in the needles [23]. The dehydration of needle tissues was reported to proceed simultaneously with the drop in F_v/F_m ratio [9]. By early October, the F_v/F_m ratio decreased to 0.25, indicating a sharp reduction in the amount of PSII complexes capable of primary charge separation and Q_A reduction. The decline in the content of photochemically active PSII centers was primarily caused by the accelerated oxidative destruction of PSII and by the impaired resynthesis of D1 protein at near-zero temperatures [5, 8, 9].

When air temperatures dropped below 0°C, the PSII completely lost its ability to reduce the PQ pool, which was evident from zero values of the parameter (1 − Vj) (Fig. 4, curve *1*). Lowering of temperature below 0°C is known to suppress the mobility of PQ in the lipid bilayer of *P. sylvestris* thylakoid membranes [24], which inhibits the electron transport between PSII and the PQ pool. Moreover, reoxidation of the acceptor side of the PSII is blocked because the PQ pool remains in the reduced state. The inhibition of PSII reoxidation may result in two-electron reduction and protonation of Q_A, which is followed by dissociation Q_A from D2 protein in the reaction center [25]. This process initiates the acceptor-type photoinhibition because the probability of $P680^+Pheo^-$ recombination increases, thus enhancing the generation of Chl P680 triplet states and singlet oxygen $^1O_2^*$. The mechanisms of energy quenching in the antenna and the reaction centers [2, 4, 11] may partly preserve the activity of PSII complexes under complete inhibition of electron transfer to the PQ pool at freezing temperatures (Fig. 4, curve *2*).

When stage 2 of frost-hardening was over at the end of the third week of October at air temperatures from −8 to −10°C, the release of free water from the cells to intercellular spaces and the concurrent formation of extracellular ice were almost completed [20]. By this time, the remaining PSII complexes completely lost their residual photochemical activity (Fig. 4) because the oxygen-evolving complex (OEC) was destroyed (Fig. 3b). The shape of the induction curve of Chl fluorescence under these conditions comprised a rapid rise to the maximum and a subsequent decrease in fluorescence (Fig. 3b). Such changes in the induction curves are known to reflect the selective inhibition of OEC in the PSII [26]. Our data are consistent with the results of Zarter et al. [6], who found that the decrease in mean daily temperatures to −10°C during winter months led to the partial degradation of OEC in the evergreen coniferous trees *Abies lasiocarpa* and *Pinus contorta* grown at 40°02′ N, 105°32′ W.

Continuous changes in irradiance, temperature, and humidity throughout the daylight period are followed by nonphotochemical quenching in the PSII antenna. The regulated *qE* component of this quenching is due to the light-induced energization of thylakoid membranes caused by lowering of the pH in the thylakoid lumen. The generation and relaxation times of the *qE* component fall into the range of seconds and minutes. The *qE* quenching comprises several key elements: the buildup of transthylakoid ΔpH, the modulation of pigment–protein complexes in the antenna, and the accumulation/activation of fluorescence quenchers (PsbS protein, Zea, Lut) [3]. These components enable the effective operation of the whole mechanism at a sufficiently wide range of temperatures and light conditions.

Our results revealed three successive phases in the seasonal dynamics of the quantum yield for NPQ ($\phi_{NPQ} \approx \phi_{qE}$) (Fig. 5): (1) a gradual increase of NPQ to the maximum values from mid-August to mid-September, (2) the retention of steady-state high NPQ at the level of 0.32–0.34 in September upon the decrease in average daily temperature from 6.4 to 1°C, and (3) a rapid decline of NPQ at the end of September, when the average daily temperature dropped to the range from 0 to −3°C. The increase in ϕ_{NPQ} in the second half of August was due to the successive phases of annual growth cycle in *P. sylvestris* when the duration

of photoperiod was reduced. When the apical meristems of needles in pine shoots enter the state of dormancy, the growth processes are arrested [13] and the photosynthetic rate decreases markedly [27]. The mean daily and night temperatures in the beginning of the second half of September were 6.2 ± 2.3 and 4.5 ± 1.7°C, respectively (Fig. 1). Busch et al. [7] observed the aggregation of LHCII trimers at nearly the same temperatures in the needles of *Pinus banksiana*. Thus, it is reasonable to suppose that the adaptive changes in macrostructural organization of antennal LHC of PSII and cyclic electron transport around PSI ensure the maintenance of high ϕ_{NPQ} values in autumn at chilling temperatures (1–10°C).

When air temperature dropped below 0°C, nonphotochemical quenching in PSII (ϕ_{NPQ}) was sharply weakened (Fig. 5). By this time, PSII completely lost the ability to reduce the PQ pool (Fig. 4, curve *1*) and, consequently, to generate the pH gradient across the thylakoid membrane. At near-zero temperatures, the constitutive (pH-independent) quenching $\phi_{f,D}$ increased dramatically (Fig. 5). The highest $\phi_{f,D}$ values were paralleled by the highest content of unregulated Zea fraction (Figs. 2 and 5). These changes provide evidence that low-temperature complex rearrangements in PSII comprise the constitutive accumulation of Zea, the aggregation of LHCII trimers, and the blockage of electron transport to the PQ pool (Fig. 4).

Thus, the results of this study and the data available in the literature provide a general view on seasonal changes in primary photosynthetic processes associated with the adaptation of *P. sylvestris* needles to extremely low winter temperatures in Central Yakutia. The rapid and comparatively early seasonal reduction in Chl content revealed in this study and the increase in Chl *a*/*b* ratio during stage 1 of frost hardening result from the degradation of the peripheral antenna of LHCII and, accordingly, from the decrease in the cross section of PSII absorption. These changes prevent the excessive absorption of light energy and ensure the balance between the primary photosynthetic reactions and carbon metabolism. The most important mechanism of short-term PSA responses, *qE* quenching in the antenna complex, is also subject to adaptation. The *qE* quenching increased simultaneously with the content of Zea when the average daily temperature dropped to 4–6°C. When stage 1 of frost hardening was replaced with the onset of stage 2 at air temperatures from 3 to –3°C, the function of PSII complexes was rapidly inactivated because of the suppressed resynthesis of D1 protein and the impaired electron transport to the PQ pool. At the same time, the content of Zea increased dramatically, and the regulated *qE* quenching was rapidly replaced by constitutive quenching involving Zea and Lut. Under the influence of lower temperatures (from –3.6 to –12.1°C) during stage 2 of frost hardening, the PSII was completely inactivated because of the disintegration of OEC. The results of this study lead us to conclude that the largest changes in the PSA occur in the narrow range of near-zero temperatures, which indicates the important role of the redox state and the PQ mobility in regulation of adaptation events and in the formation of frost resistance of needles.

ACKNOWLEDGMENTS

This work was supported by the Russian federal budget according to the research programs of the Institute for Biological Problems of the Cryolithozone, Siberian Branch, Russian Academy of Sciences (registration no. AAAA-A17-117020110054-6) and the Institute of Biology, Komi Research Center, Ural Branch, Russian Academy of Sciences (registration no. AAAA-A17-117033010038-7). T.K. Antal is grateful to the Russian Science Foundation (project no. 14-50-00029) for the support in analysis and discussion of JIP tests and for taking part in writing the paper.

REFERENCES

1. Chang, C.Y., Fréchette, E., Unda, F., Mansfield, S.D., and Ensminger, I., Elevated temperature and CO_2 stimulate late-season photosynthesis but impair cold hardening in pine, *Plant Physiol.*, 2016, vol. 172, pp. 802–818.
2. Ensminger, I., Busch, F., and Huner, N.P.A., Photostasis and cold acclimation: sensing low temperature through photosynthesis, *Physiol. Plant.*, 2006, vol. 126, pp. 28–44.
3. Ruban, A.V., Johnson, M.P., and Duffy, C.D.P., The photoprotective molecular switch in the photosystem II antenna, *Biochim. Biophys. Acta*, 2012, vol. 1817, pp. 167–181.
4. Ivanov, A.G., Sane, P.V., Zeinalov, Y., Simidjiev, I., Huner, N.P.A., and Oquist, G., Seasonal responses of photosynthetic electron transport in Scots pine (*Pinus sylvestris* L.) studies by thermoluminescence, *Planta*, 2002, vol. 215, pp. 457–465.
5. Ottander, C., Campbell, D., and Oquist, G., Seasonal-changes in photosystem II organization and pigment composition in *Pinus sylvestris, Planta*, 1995, vol. 197, pp. 176–183.
6. Zarter, C.R., Adams, W.W., Ebbert, V., Cuthbertson, D.J., Adamska, I., and Demmig-Adams, B., Winter down-regulation of intrinsic photosynthetic capacity coupled with up-regulation of Elip-like proteins and persistent energy dissipation in a subalpine forest, *New Phytol.*, 2006, vol. 172, pp. 272–282.
7. Busch, F., Huner, N.P.A., and Ensminger, I., Increased air temperature during simulated autumn conditions does not increase photosynthetic carbon gain but affects the dissipation of excess energy in seedlings of the evergreen conifer jack pine, *Plant Physiol.*, 2007, vol. 143, pp. 1242–1251.
8. Verhoeven, A., Osmolak, A., Morales, P., and Crow, J., Seasonal changes in abundance and phosphorylation

status of photosynthetic proteins in eastern white pine and balsam fir, *Tree Physiol.*, 2009, vol. 29, pp. 361–374.

9. Verhoeven, A., Sustained energy dissipation in winter evergreens, *New Phytol.*, 2014, vol. 201, pp. 57–65.
10. Sofronova, V.E., Chepalov, V.A., Dymova, O.V., and Golovko, T.K., Photoprotective mechanisms in photosystem II of *Ephedra monosperma* during development of frost tolerance, *Russ. J. Plant Physiol.*, 2014, vol. 61, pp. 751–759.
11. Sofronova, V.E., Dymova, O.V., Golovko, T.K., Chepalov, V.A., and Petrov, K.A., Adaptive changes in pigment complex of *Pinus sylvestris* needles upon cold acclimation, *Russ. J. Plant Physiol.*, 2016, vol. 63, pp. 433–442.
12. Savitch, L.V., Ivanov, A.G., Krol, M., Sprott, D.P., Oquist, G., and Huner, N.P.A., Regulation of energy partitioning and alternative electron transport pathways during cold acclimation of Lodgepole pine is oxygen dependent, *Plant Cell Physiol.*, 2010, vol. 51, pp. 1555–1570.
13. Sudachkova, N.E., Girs, G.I., Prokushkin, S.G., Antonova, G.F., Varaksina, T.N., Kaverzina, L.N., Kozhevnikova, N.N., Kozlova, L.N., Kolovskii, R.A., Kudashova, F.N., Menyailo, L.N., Milyutina, I.L., Osipov, V.I., Romanova, L.I., Semenova, G.P., et al., *Fiziologiya sosny obyknovennoi* (Physiology of Scots Pine), Novosibirsk: Nauka, Sib. Otd., 1990.
14. Strasser, R.J., Tsimilli-Michael, M., and Srivastava, A., Analysis of chlorophyll *a* fluorescence transient, in *Chlorophyll Fluorescence: A Signature of Photosynthesis*, Papageorgiou, G. and Govindjee, Eds., Dordrecht: Kluwer, 2005, pp. 321–362.
15. Klughammer, C. and Schreiber, U., Complementary PS II quantum yields calculated from simple fluorescence parameters measured by PAM fluorometry and the Saturation Pulse method, *PAM Application Notes*, 2008, vol. 1, pp. 27–35.
16. Lichtenthaler, H.K., Chlorophylls and carotenoids: pigments of photosynthetic biomembranes, in *Methods in Enzymology*, Colowick, S.P. and Kaplan, N.O., Eds., San Diego: Academic, 1987, vol. 148, pp. 350–382.
17. Gilmore, A.M. and Yamamoto, H.Y., Resolution of lutein and zeaxanthin using a non-endcapped, lightly carbon loaded C18 high performance liquid chromatographic column, *J. Chromatogr.*, 1991, vol. 35, pp. 67–78.
18. Antal, T. and Rubin, A., In vivo analysis of chlorophyll *a* fluorescence induction, *Photosynth. Res.*, 2008, vol. 96, pp. 217–226.
19. Klimov, S.V., Plants adaptation to stresses through donor-acceptor relations on different levels of structural organization, *Usp. Sovrem. Biol.*, 2008, vol. 128, pp. 282–300.
20. Tumanov, I.I., *Fiziologiya zakalivaniya i morozostoikosti rastenii* (Physiology of Hardening and Frost Resistance of Plants), Moscow: Nauka, 1979.
21. Oquist, G. and Huner, N.P.A., Photosynthesis of overwintering evergreen plants, *Annu. Rev. Plant Biol.*, 2003, vol. 54, pp. 329–355.
22. Sato, R., Ito, H., and Tanaka, A., Chlorophyll *b* degradation by chlorophyll *b* reductase under high-light conditions, *Photosynth. Res.*, 2015, vol. 126, pp. 249–259.
23. Tatarinova, T.D., Perk, A.A., Bubyakina, V.V., Vasil'eva, I.V., Ponomarev, A.G., and Maksimov, T.Kh., Dehydrin stress proteins in *Pinus sylvestris* L. needles under conditions of extreme climate of Yakutia, *Dokl. Biochem. Biophys.*, 2017, vol. 473, no. 1, pp. 98–101.
24. Oquist, G., Seasonally induced changes in acyl lipids and fatty acids of chloroplast thylakoids of *Pinus sylvestris, Plant Physiol.*, 1982, vol. 69, pp. 869–875.
25. Richter, M., Rhule, W., and Wild, A., Studies on the mechanism of photosystem II photoinhibition. II. The involvement of toxic oxygen species, *Photosynth. Res.*, 1990, vol. 24, pp. 237–243.
26. Strasser, B., Donor side capacity of photosystem II probed by chlorophyll *a* fluorescence transients, *Photosynth. Res.*, 1997, vol. 52, pp. 147–155.
27. Vogg, G., Heim, R., Hansen, J., Schafer, C., and Beck, E., Frost hardening and photosynthetic performance of Scots pine (*Pinus sylvestris* L.). I. Seasonal changes in the photosynthetic apparatus and its function, *Planta,* 1998, vol. 204, pp. 193–200.

Translated by A. Bulychev